JOINT INSTITUTE FOR NUCLEAR RESEARCH

Flerov Laboratory of Nuclear Reactions

FINAL REPORT ON THE
INTEREST PROGRAMME

Cryogenic gas stopping cell

Supervisor:
Dr. Lubos Krupa

Student:
Indu Jangid, Indian Institute of
Technology Roorkee, Roorkee, India

Participation Period:
May 24 - July 02, Wave 04
Dubna, 2021

Acknowledgements

I would like to take this opportunity to express my sincere gratitude, sense of indebtedness to my Supervisor Dr Lubos Krupa, for his inspiring guidance and meticulous supervision throughout my project work, providing all the information related to this project and answers all my queries. The entire report is structured and formulated based on his instructions and guidelines. I am extremely grateful to the interest team and university center of JINR to start this program and allow me to participate in this.

Abstract

Low-energy radioactive ion beams are a prerequisite for many precision experiments in nuclear physics. The efficient transformation of rare ion beams, produced in nuclear reactions at high energy with large emittance, into low-energy beams with small emittance and low energy spread was a challenge since the first accelerators. In recent years, so-called ion-catcher devices (gas stopping cells) have been employed to decelerate high-energy ions in a noble-gas atmosphere, from where they are extracted by gas flow and electric fields. The cryogenic gas stopping cell is developed, realized and tested at cyclotron DC280 ("Factory of Superheavy Elements") to study the properties of heavy and superheavy elements.

Contents

Chapter 1

Introduction

SHIPTRAP is a double Penning-trap mass spectrometer at the GSI Darmstadt, Germany, positioned behind the separator for heavy-ion reaction products (SHIP) at the end of the universal linear accelerator (UNILAC). It is perfect for direct high-precision mass measurements of the heavier elements generated in fusion-evaporation nuclear reactions. This mass spectrometry (PTMS) necessitates the ion of interest being stopped, thermalized, and prepared. Gas cells are capable of completing this task with limited efficiency. Ions are slowed down by inelastic collisions in a pure inert gas volume, resulting in charge exchange processes. This technique was initially used on fusion evaporation reaction products at the Ion-Guide Isotope-Separator On-Line (IGISOL) facility in 1985. PTMS was expanded to heavy nuclei, in the pioneering experiment, with production rates as low as a few ions per minute. The drop in production rate must be balanced by a rise in efficiency and setup sensitivity. Hence, to make direct mass measurements of super-heavy elements (Z > 104), it is necessary to improve the overall efficiency of the setup, and thus the efficiency of the buffer-gas stopping cell at SHIPTRAP.

To that aim, a second-generation cryogenic gas-stopping cell (CGC) or CryoCell has been created at SHIPTRAP. This stopping cell operate at cryogenic temperature. The CryoCell has several advantages, including an immense stopping volume, a lower 'dead' volume owing to coaxial injection. To optimize the mass resolving power and precision of SHIPTRAP, the highest possible charge state that can withstand the following room-temperature buffer-gas in the buncher section and the preparation trap is preferred. In most cases, this corresponds to a doubly-charged state. The CGC has required rearranging the entire beamline from a perpendicular to a close-to-zero-degree position concerning SHIP.

The CGC is an essential part of the SHIPTRAP setup, allowing mass measurements in the zone of the heaviest elements. Since the synthesis rates for these elements are limited and the total particle integral is low, the CGC must run as efficiently as feasible. Furthermore, the stopping and extraction efficiency from the CGC must be quick enough to avoid any additional ion losses due to the EVRs' finite half-lives.
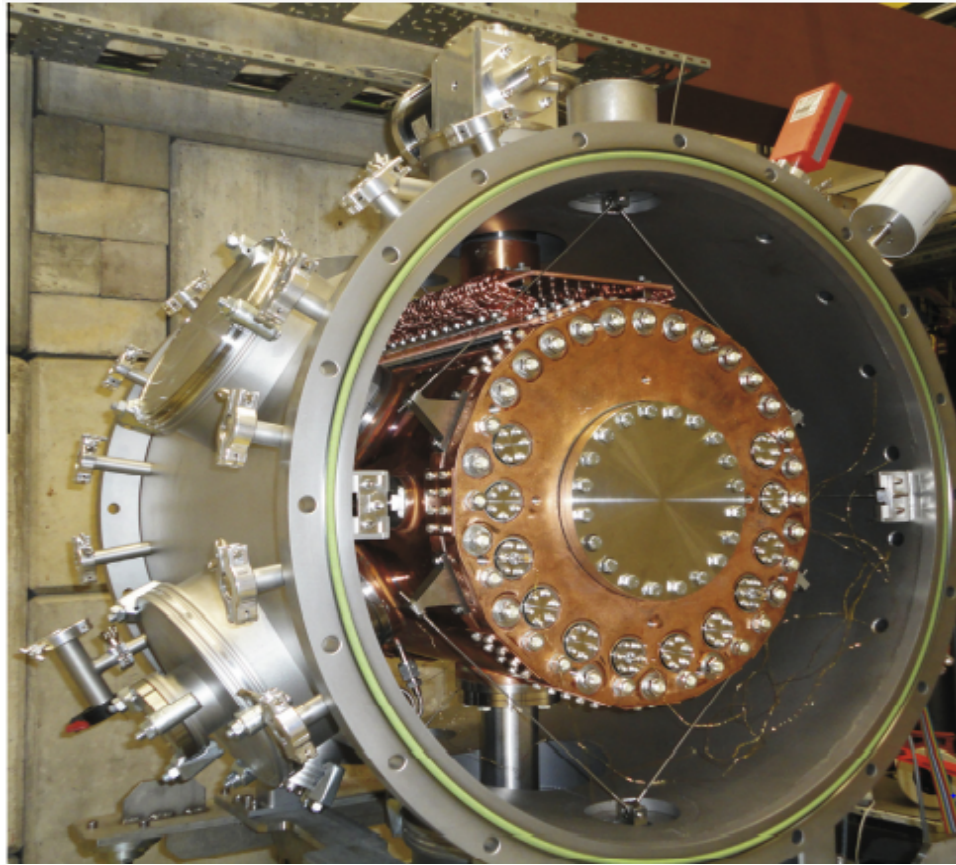
Figure 1.1: Cryogenic gas stopping cell

1.1. Cryogenic gas stopping cell

A figure of cryogenic gas stopping cell is shown in Fig. 1.1. The cryogenic gas stopping cell has a chamber, filled with ultra-pure He gas at pressures of approximately 50 mbar. This chamber is situated inside an evacuated chamber containing multi-layer insulation foils and it can be cooled down to 40 K using a cryo cooler.

Energetic ions are thermalized in a noble gas, in the stopping cell. After slowing down, the chance of an ion being in an ionic state ranges from tens to more than fifty percent, which is big enough to be useful. Due to the high ionisation potential of noble gas atoms, ions cannot neutralise in collisions with them near and at thermal energy. As a result, if the circumstances are right, these ions can survive long enough to be transported out of the stopping volume through an exit hole and then formed into a low-energy ion beam. Low-energy radioactive ion beams are a prerequisite for many precision experiments in nuclear physics.

1.1.1 Setup

The setup of cryogenic gas stopping cell shown in Fig. 1.2. There are two stainless steel chambers that make up the CryoCell:

- The outer vacuum chamber; provides a thermal insulation and includes a multi-layer insulation foil to prevent heat transmission to the inner chamber.

- The inner chamber; is copper-plated on the outside with a 2 mm thick coating of copper and is cooled to around 40 K using a cryo cooler.

During cooling and warming stages, the copper layer provides a uniform temperature distribution across the CryoCell.
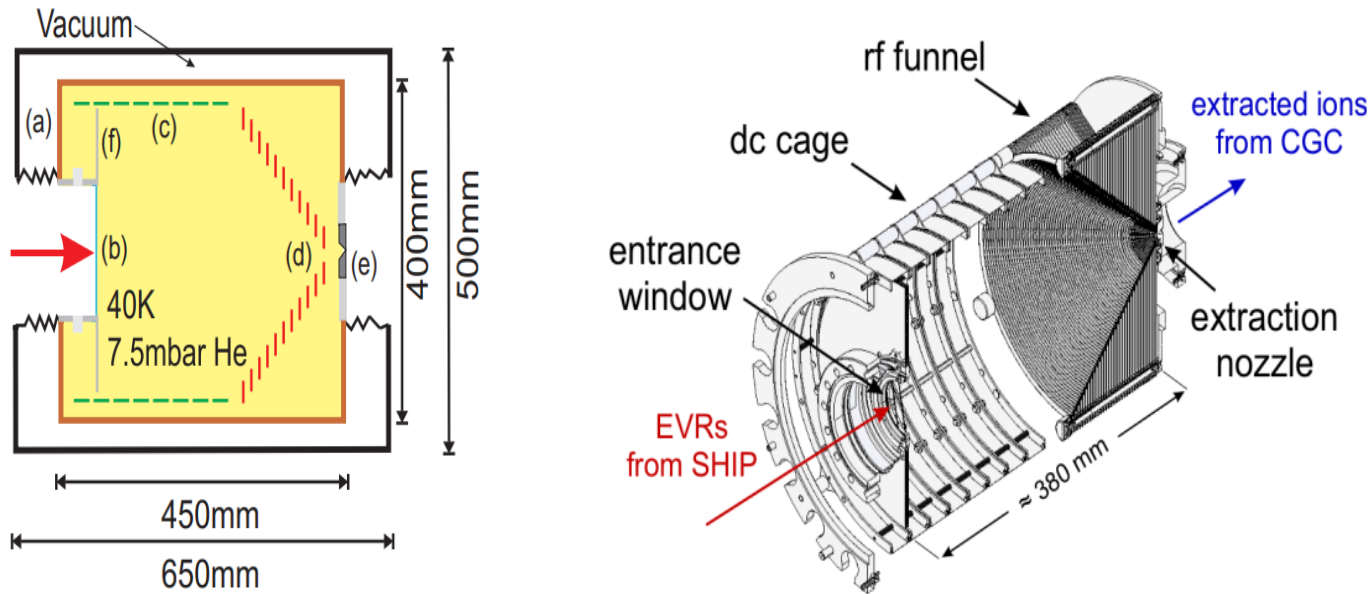

Figure 1.2: Setup of the Cryogenic gas stopping cell

In the figure:
(a) the outer chamber
(b) the entrance window
(c) the electrostatic cage
(d) the radio-frequency funnel structure
(e) the extraction nozzle
(f) disc electrode

The so-called entrance window ((b) in Fig. 1.2) is placed on one end edge of the inner chamber. This window is electrically isolated from the inner chamber and may thus be treated as an electrode at particular voltages. The thickness of the entrance

window is such that energetic beam particles lose 90% of their energy when they enter the inner chamber through it. The beam particles are further decelerated after passing through the entrance window due to interactions with the helium buffer-gas atoms. An electrode system, the DC cage, is placed on the same end flange of the inner chamber. The DC cage's electrostatic field guides the thermalized ions through the buffer gas to the extraction region. An electrode structure known as an RF funnel is put on the opposing end flange, to which an RF voltage, as well as a DC voltage gradient, may be supplied to produce a repulsive force that inhibits ions from reaching the electrodes. The RF funnel directs the ions towards the CryoCell's exit by focusing them onto the beam axis. The ions are extracted from the CryoCell in a supersonic gas jet through the extraction nozzle after passing through the RF funnel. For the extraction of positively charged ions, the extraction nozzle is electrically insulated, and a few volts' negative potential is supplied.

1.1.2 Optimization of the Stopping Efficiency

In the PTMS of the heaviest elements, stopping and thermalization of the incoming fusion-evaporation residuals (EVRs) is a crucial aspect. Because incoming ion rates and particle integrals are generally modest, this must be as efficient as feasible. Any loss should be avoided as PTMS needs at least a few ions for a measurement. The stopping efficiency given by

$$\epsilon_{stop} = \frac{n_{stopped}}{n_{inc}\epsilon_{geom}}. \tag{1.1}$$

Where n_{inc} is the incoming ions, and $n_{stopped}$ are the ions which are stopped in the active gas volume of the CryoCell. And

$$\epsilon_{geom} = (1 - n_{geom}) \tag{1.2}$$

ϵ_{geom} represents the geometrical efficiency (the fraction of ions which do not hit the entrance window n_{geom}).
The kinetic energy of the incident EVR, the entrance window foil type and thickness, as well as the buffer-gas type and density of the CGC, all influence stopping efficiency. The only ions that can be extracted are those that are stopped inside the CGC's active gas volume. However, the energy loss through the entrance window foil must be high enough for the buffer-gas density to be sufficient for stopping.
The stopping efficiency for EVRs are calculated using the Stopping and Range of Ions in Matter (SRIM) software package.

1.2. SRIM Software

Stopping and Range of Ions in Matter (SRIM) is a collection of computer programmes that calculate the interaction of ions with matter; the programme Transport of Ions

in Matter (TRIM) is the core of SRIM. SRIM is widely used in other fields of radiation material science and is popular in the ion implantation research and technology community. It is a semi-empirical Monte Carlo code which is based on binary collision model, and it has been parametrized using experimental data. It uses the Ziegler-Biersack-Littmar model to compute the average charge state in matter and uses an effective charge for the projectile. It requires the ion type and energy (in the range 10 eV – 2 GeV) as input parameters, as well as the material of one or more target layers. With an overall accuracy of better than 4%, SRIM can reproduce the stopping powers of about 25000 experimental data points. If projectile parameters are adjusted to represent the stopping of heavier ions, SRIM gives a wonderful chance to estimate and optimise the entrance window foil material, thickness, and buffer gas type and density for a variety of EVRs.

Chapter 2

Results and discussion

Fig. 2.1 shows the stopping efficiency distribution for radon isotope produced in complete fusion reaction ^{44}Ar + ^{144}Sm, as a function of the titanium entrance window foil thickness. Simulation's are being carried out using the SRIM software at room temperature and gas pressures of 30 mbar, 50 mbar, 70 mbar, and 100 mbar.
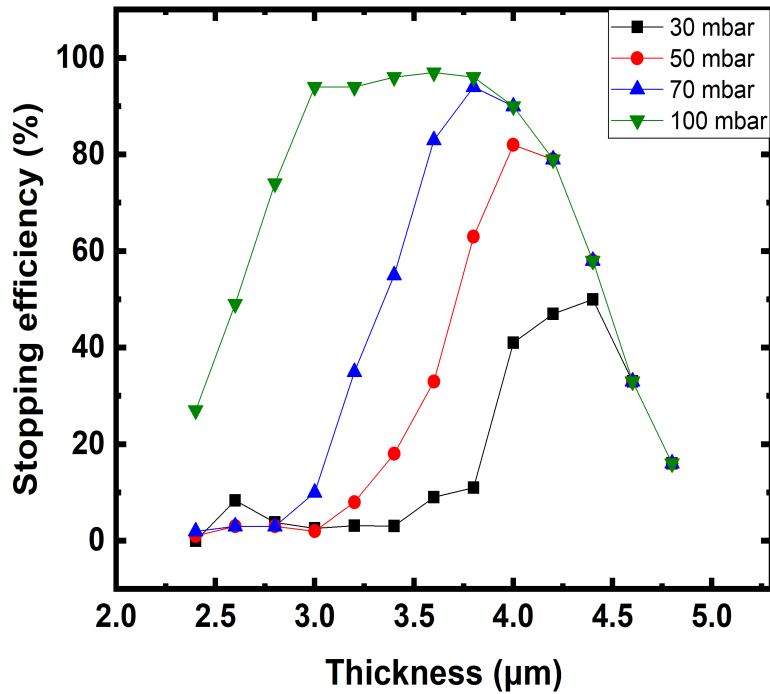

Figure 2.1: Stopping efficiency distribution for radon isotopes

Here the thickness of the titanium foil is varying from 3.2 μm to 4.8 μm and in this the simulations have done by taking the difference of 0.2 μm.

Here the helium gas environment is taken. It has been observed that on increasing the pressure stopping efficiency is also increases and it is almost same when the thickness of the titanium foil reaches 4.2 μm. In this simulation the energy of the ion is not constant it has Gaussian distribution within range 35 MeV to 45 MeV. The energy distribution for radon particle is shown in Fig. 2.2.
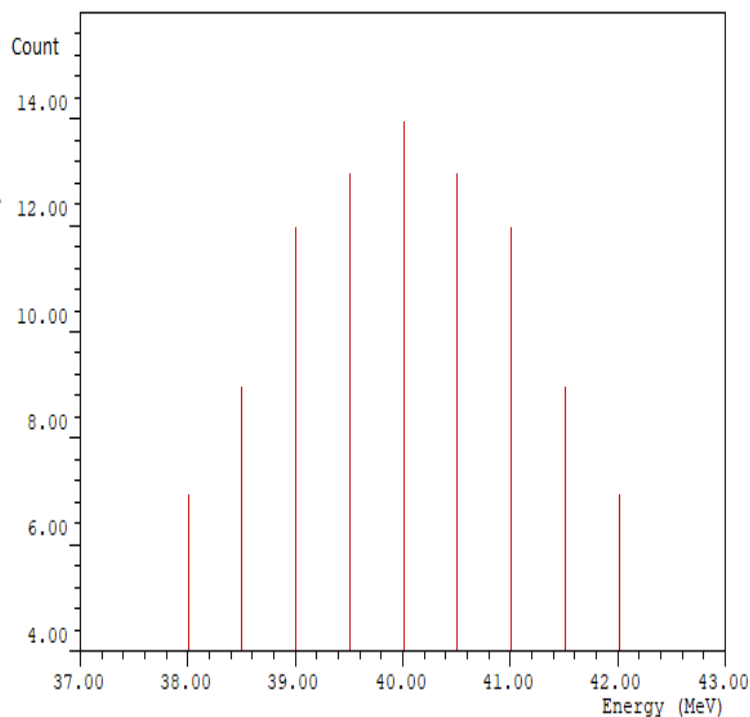

Figure 2.2: Energy distribution

Input parameters in the SRIM software for the above simulation are as follows:
He Gas Pressure mbar
Pressure = 30/50/70/100
Temperature = 300
He density = 0.00000481/0.00000802/0.00001122 (g/cm^3)

Ti thickness in μ
ThicknessFrom = 2.4
ThicknessStep = 0.2
ThicknessAmount = 13

Source Radius
IsotopRadius = 25
R_MIN_MAX = 0.5

Ion properties
IonZ = 86
IonAtomicMass = 205

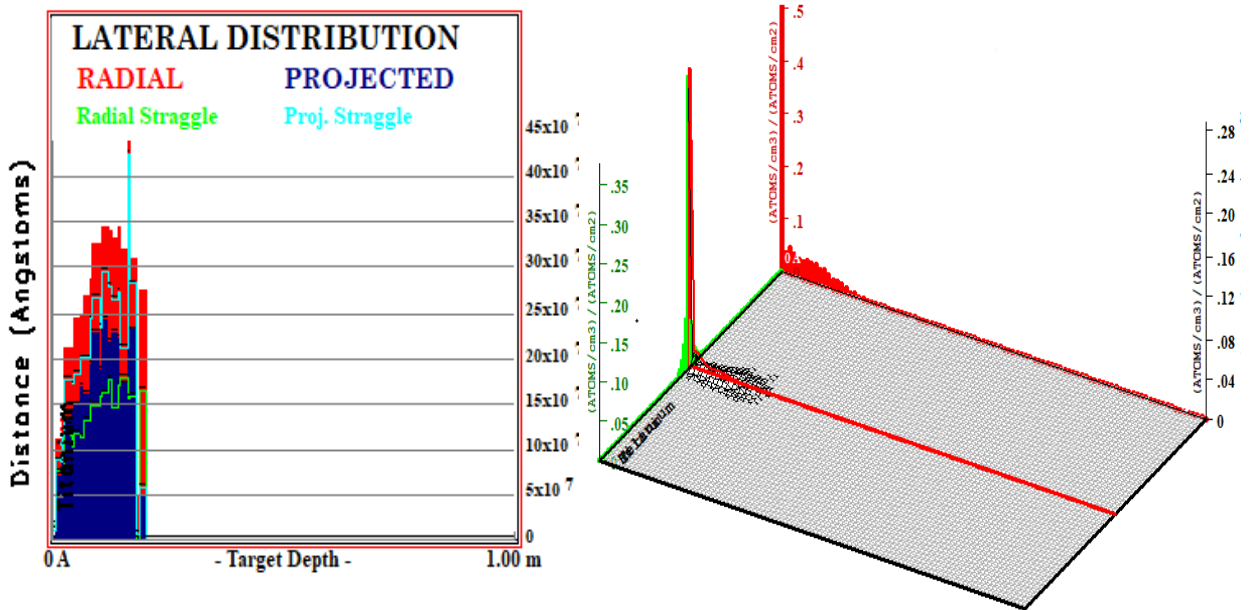**Ion Energy distribution**
IGaussDistrib = 1
ISumAll = 100
IBins = 10
IEmiddle = 40
IE_MIN_MAX = 0.3
IEWidth = 5

The simulations have been performed for ^{205}Rn ion at different energies. The radon particles passes through the titanium foil of fix thickness 4.5 μm in an helium environment with different pressure and fixed temperature 300 K.
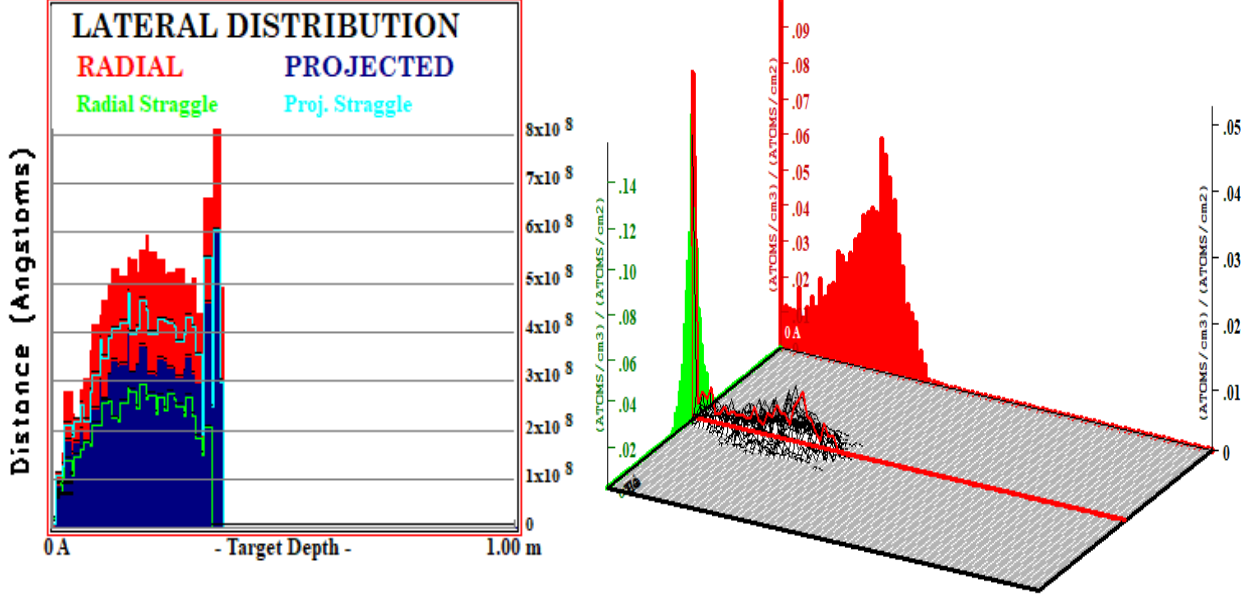

(a) Lateral Spread of Ions   (b) 3-Dimensional Ion Range Distributions

Figure 2.3: For ^{205}Rn at 40 MeV and pressure at 70 mbar

Figs. 2.3, 2.4, and 2.5 are obtained by the simulations which have done at the kinetic energy of 40 MeV, 50 MeV, and 60 MeV of radon ion and at pressure 70 mbar, 56 mbar, and 70 mbar of helium gas respectively. Here Fig. (a) shows the lateral spread of the ions from the original ion axis. Both the first moment of the spread (solid plots) and the second moment, the straggle, of the spread (line plots) are shown. The lateral projected range is defined as the average of the absolute values of the projected lateral

displacements from the X-axis. And the Radial Range is the mean radial displacement range from the X-axis assuming cylindrical symmetry.

(a) Lateral Spread of Ions   (b) 3-Dimensional Ion Range Distributions

Figure 2.4: For ^{205}Rn at 50 MeV and pressure at 56 mbar

Table 2.1: Calculated statistical quantities from the 3-Dimensional Ion Range Distributions

^{205}Rn			
Kinetic energy (MeV)	40	50	60
Pressure (mbar)	70	56	70
Ion Ranges (mm)	32.1	177	364
Skewness	1.282	-0.571	-1.489
Straggle (mm)	45.4	91.8	108
Kurtosis	3.523	2.286	5.053

Many applications require more elaborate 3-Dimesional (3-D) distributions, for example might be an analysis in the semiconductor technology. Fig. (b) represents the 3-Dimensional Ion Range Distributions for radon paticle. Here the ions are tabulated with their X (depth), Y and Z (lateral) coordinates. The red graph for the 2-D depth plot and the green graph for the 2-D lateral plot. Here in this figure we calculated the Straggling, Skewness and Kurtosis which are names for statistical quantities related to the second, third and forth moments of the ion distribution. These values are shown
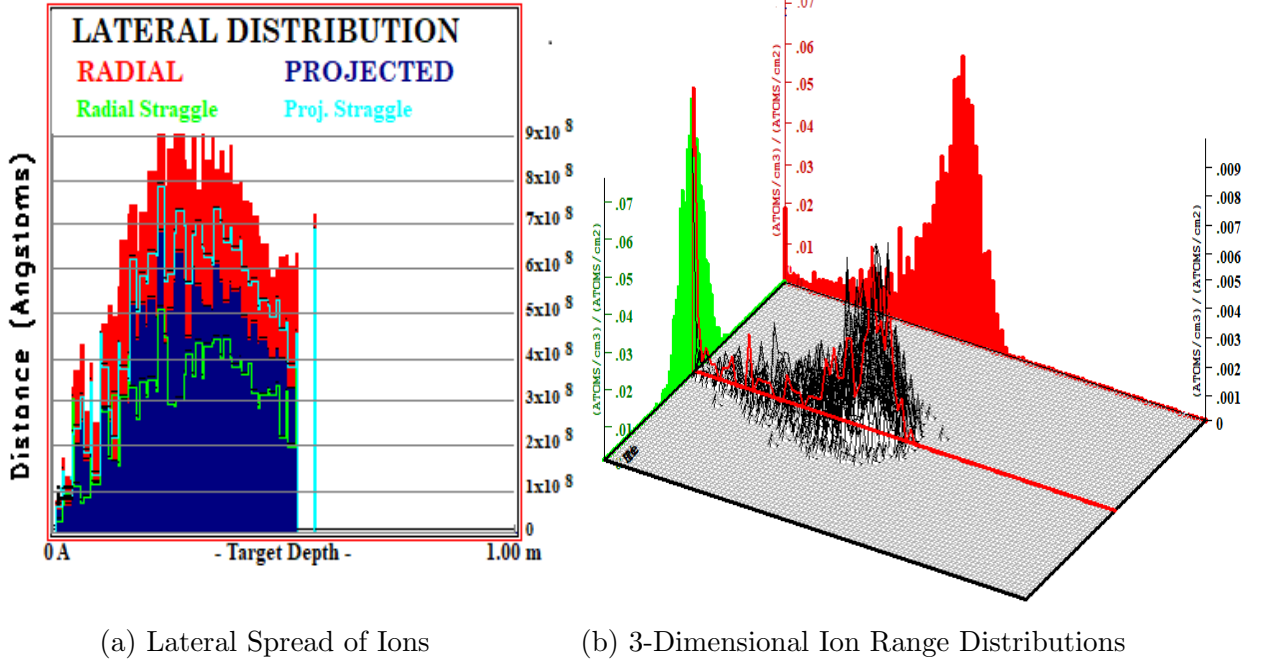
(a) Lateral Spread of Ions   (b) 3-Dimensional Ion Range Distributions

Figure 2.5: For ^{205}Rn at 60 MeV and pressure at 70 mbar

in the Table 1. "Straggling" is a word which is used in ion implantation. It is define as the square root of the variance:

$$Straggling = (\sigma) = [(\sum_i x_i^2)/N - R_p^2] = < (\Delta x_i)^2 >^{1/2} \qquad (2.1)$$

Where R_p is the mean projected range

$$R_p = \sum_i x_i/N = < x > \qquad \& \qquad (2.2)$$

$$\Delta x_i = (x_i - R_p) \qquad (2.3)$$

Here x_i is the projected range of ion "i" on the x-axis and N is the number of ions. And the Skewness and Kurtosis is defined by respectively:

$$Skewness = \gamma = < \Delta x^3 > / < \Delta x^2 >^{3/2}, \qquad (2.4)$$

$$Kurtosis = \beta = < \Delta x^4 > / < \Delta x^2 >^2 . \qquad (2.5)$$

The projected range and the straggling have dimensions of length and skewness, and kurtosis, are dimensionless. The skewness tells whether the peak is skewed towards the surface (negative values) or away from the surface (positive values) and Kurtosis indicates the extent of the distribution tails.

Chapter 3

Conclusion

Stopping efficiency for ^{205}Rn is calculated at four different pressures by varying the titanium foil thickness and energy of the incident ion. We have observed that on increasing the thickness of titanium foil stopping efficiency first increases and after reaching the maximum it start decreasing with increasing the thickness of titanium foil. It can be said that stopping efficiency becomes the same at higher thickness. The simulations suggest a change in the entrance window foil thickness of 0.2 µm with respect to its optimial value which results into a drop in the stopping efficiency of about 20 % (absolute).

The Lateral spread of the ion and 3-dimensional ion range distribution is also shown for the radon. This distribution is shown at ion energy 40 MeV, 50 MeV, and 60 MeV and at pressure 70 mbar, 56 mbar, and 70 mbar of helium gas respectively. All of the simulations have been performed at room temperature.

Bibliography

[1] M. Ranjan, P. Dendooven, S. Purushothaman, et al.,Nucl. Instrum. Methods. Phys. Res. A **770** (2015) 87.

[2] O. Kaleja, B. Andelic, K. Blaum, et al., Nucl. Instrum. Methods. Phys. Res. B **463** (2020) 280.

[3] C. Droese, S. Eliseev, K. Blaum, et al., Nucl. Instrum. Methods. Phys. Res. B **338** (2014) 126.

[4] Oliver T. Kaleja, High-precision mass spectrometry of nobelium, lawrencium and rutherfordium isotopes and studies of long-lived isomers with SHIPTRAP. Diss. Johannes Gutenberg-Universität Mainz Mainz, 2020.

[5] http://www.srim.org/

[6] J. F. Ziegler, M. D. Ziegler, and J. P. Biersack, NUCL INSTRUM METH B **268** (2010) 1818.